Journal of Agriculture and Rural Development in the Tropics and Subtropics
Vol. 111 No. 2 (2010) 129-142

urn:nbn:de:hebis:34-2011052737598 ISSN: 1612-9830 – journal online: www.jarts.info

Assessment of land use and land cover changes during the last 50 years in oases and surrounding rangelands of Xinjiang, NW China

Andreas Dittrich , Andreas Buerkert , Katja Brinkmann*

Organic Plant Production and Agroecosystems Research in the Tropics and Subtropics, University of Kassel, Witzenhausen, Germany

Abstract

An analysis of historical Corona images, Landsat images, recent radar and Google Earth® images was conducted to determine land use and land cover changes of oases settlements and surrounding rangelands at the fringe of the Altay Mountains from 1964 to 2008. For the Landsat datasets supervised classification methods were used to test the suitability of the Maximum Likelihood Classifier with subsequent smoothing and the Sequential Maximum A Posteriori Classifier (SMAPC). The results show a trend typical for the steppe and desert regions of northern China. From 1964 to 2008 farmland strongly increased (+ 61 %), while the area of grassland and forest in the floodplains decreased (- 43 %). The urban areas increased threefold and 400 ha of former agricultural land were abandoned. Farmland apparently affected by soil salinity decreased in size from 1990 (1180 ha) to 2008 (630 ha). The vegetated areas of the surrounding rangelands decreased, mainly as a result of overgrazing and drought events.

The SMAPC with subsequent post processing revealed the highest classification accuracy. However, the specific landscape characteristics of mountain oasis systems required labour intensive post processing. Further research is needed to test the use of ancillary information for an automated classification of the examined landscape features.

Keywords: Altay Mountains, LUCC, Landsat, Corona, NDVI, SMAPC, MLC

Abbreviations:
SMAPC = Sequential Maximum A Posteriori Classifier
NDVI = Normalized Difference Vegetation Index
MLC = Maximum Likelihood Classifier
LUCC = Land use and land cover changes
GCPs = Ground Control Points

1 Introduction

During the last decades many landscapes have undergone large structural changes given the introduction of new management practices and the social, political, and economic framework controlling land use (di Castri & Hadley, 1988; Turner *et al.*, 2001). In China, such processes have reportedly resulted in widespread land degradation, often caused by population growth and over-intensification of agriculture such as excessive application of mineral fertilizers, overgrazing of steppes and excessive cutting of trees and shrubs for fuel wood (Zhu & Chen, 1994), man-made salinisation and losses of wetlands (Zhang *et al.*, 2007). Climate change effects (Hu *et al.*, 2003) are also claimed as recent drivers of land use change (Goa *et al.*, 2002; Klein *et al.*, 2004).

In the arid parts of NW China the state and development of oasis systems are of particular importance given their dominant role in many landscapes of the Xinjiang-Uyghur Autonomous Region (Liu *et al.*, 2010). During the last 50 years the population of this part of China increased from 4.7 to 18.5 Mio. people and the area of cultivated land expanded from 1.5 to 3.4 million ha (Wiemer, 2004). Collectivisation programs fostered the conversion of grassland into cropland and of herders into agro-pastoralists (Millward & Tursun, 2004; Chuluun & Ojima, 2002). As a result of poor reclamation of land, decreasing pasture areas, inefficient livestock husbandry systems and rising demand of meat due to rapid population growth and changes in food consump-

*Corresponding author
Fax +49 5542-98 1230; Email: tropcrops@uni-kassel.de

tion preferences, the grazing pressure on the remaining rangeland areas increased dramatically (Liu, 1993; Graetz, 1994; Li *et al.*, 2008). Since the 1980s, most of the oases in Xinjiang are characterized by mechanized cropping systems that depend on an intensive use of irrigation water accompanied by often insufficient drainage (Zhang *et al.*, 2001; Bruelheide *et al.*, 2003; Graefe *et al.*, 2004). As a consequence, land degradation through salinisation and sand encroachment increased (Brunner, 2005; Xiuling, 2001). In 2000 about 50 % of the total river water in Xinjiang was used for oasis irrigation leading to a rise of salt content in rivers and lakes (Li *et al.*, 2001).

To detect and monitor land use and land cover changes (LUCC) and ongoing desertification processes, satellite remote sensing, in conjunction with geographic information systems (GIS), has been widely applied and been recognized as a powerful analytical tool (Xiaoa *et al.*, 2004; Jia *et al.*, 2004; Zhang *et al.*, 2007).

For China, however, most LUCC studies examined steppe and desert regions and only rarely targeted complex oasis systems (Hao & Ren, 2009; Luo *et al.*, 2008; Li *et al.*, 2004). These studies were either based on visual image interpretation or on automated classification algorithms. Other remote sensing studies in China have been conducted to monitor desertification processes (Hill, 2001; Baoping & Tianzong, 2001), quantify rangeland biomass production (Runnström, 2003), map vegetation types (Wang *et al.*, 2002), and to analyse the temporal and spatial development of urban areas (Jun *et al.*, 2006). In contrast to the described studies, our work focused on LUCC in complex oasis systems at the foothills of the Altay Mountains. The objectives of the study were (i) to determine LUCC of oasis systems and their surrounding rangelands in the Altay Mountains between 1964 and 2008 using remote sensing techniques and (ii) to evaluate the effectiveness of automated procedures to determine land use and land cover changes at a broader scale. In this context, the suitability of the commonly used 'Maximum Likelihood Classifier' (MLC) with subsequent smoothing (Pal & Mather, 2003; Booth & Oldfield, 1989) and the rarely used 'Sequential Maximum A Posteriori Classifier' (SMAPC, Bouman & Shapiro, 1994) were compared. The latter approach is often more accurate when classifying different types of crops cultivated on homogenous fields (McCauley & Engel, 1995).

2 Materials and Methods

2.1 Study area

The study area is located in Qinghe County in the NW part of the Dzungarian basin in the Xinjiang Autonomous Region of China (Figure 1). The basin is surrounded by the Altay range in the north and the Tianshan mountains in the south. The 482 km^2 study area (90°15'30" – 90°30'30" E and 46°24'30" – 46°48'30" N) encompasses several oasis settlements at altitudes between 1185 and 1890 m a.s.l, including the town of Qinghe in the South and the village Buheba in the North (Figure 2 and 3). From 1962 to 1997, the mean temperature in Qinghe county was 1.1°C with a mean annual precipitation of 40 – 80 mm (NCDC, 2009). Given the short vegetation period, spring wheat (*Triticum aestivum* L.) is the dominant crop, which, after sowing in April is widely grazed to foster tillering. Intensive greenhouse vegetable production as an alternative to the cultivation of irrigated spring wheat only occurs in the immediate proximity of or within oasis settlements. At present an unknown number of (agro-) pastoralists practice summer transhumance, while the reminder reportedly managing about 30-40 % of Qinghe's livestock, remain in the agricultural area throughout the year with daily grazing in the neighbourhood of the oasis area.

Since 2002, the local government has implemented a forest policy, reconverting degraded arable land into pasture or forest. Under this policy so far, 8,600 ha have been reforested, and 3,800 ha of the reclaimed poplar (*Populus* sp.) forest area are protected from grazing by fences. In addition, 40,000 ha of original forest in the north of Qinghe county have been put under protection.

2.2 Data acquisition and pre-processing

To identify LUCC that occurred from 1964 to 2008 in the study area, different satellite image sources were used, such as Corona, Landsat, Google Earth® images, and TerraSAR-X (Synthetic Aperture Radar) radar images (Table 1). The earliest data resulted from two panchromatic Corona (KH-4B) images taken in 1964 by the U.S Geological Survey's Earth Resources Observation and Science (EROS). During the Corona program from 1960-1972, several camera systems, referred to by their KEYHOLE (KH) designator, were used. Of these the most advanced, KH-4B had its best resolution of 1.8 m at nadir. We further obtained cloud free Landsat 5 and 7 Level 1 terrain corrected images (L1T, resolution = 30 m) from EROS, which have radiometric, geographic and topographic corrections. Since 2003, Landsat 7 imagery has been interrupted and contains data gaps due to the failure of the Scan Line Corrector (SLC), which compensates for the forward motion of the satellite (Chander *et al.*, 2009). Thus, an already processed, gap-filled product was obtained to accurately depict the land use and land cover conditions in August 2008.

All Landsat images covered the whole study area. The two TerraSAR-X radar images displayed 85 % of the oasis and 25 % of the surrounding area, while the Google Earth® Quickbird images covered a total of 89 % of the study area.

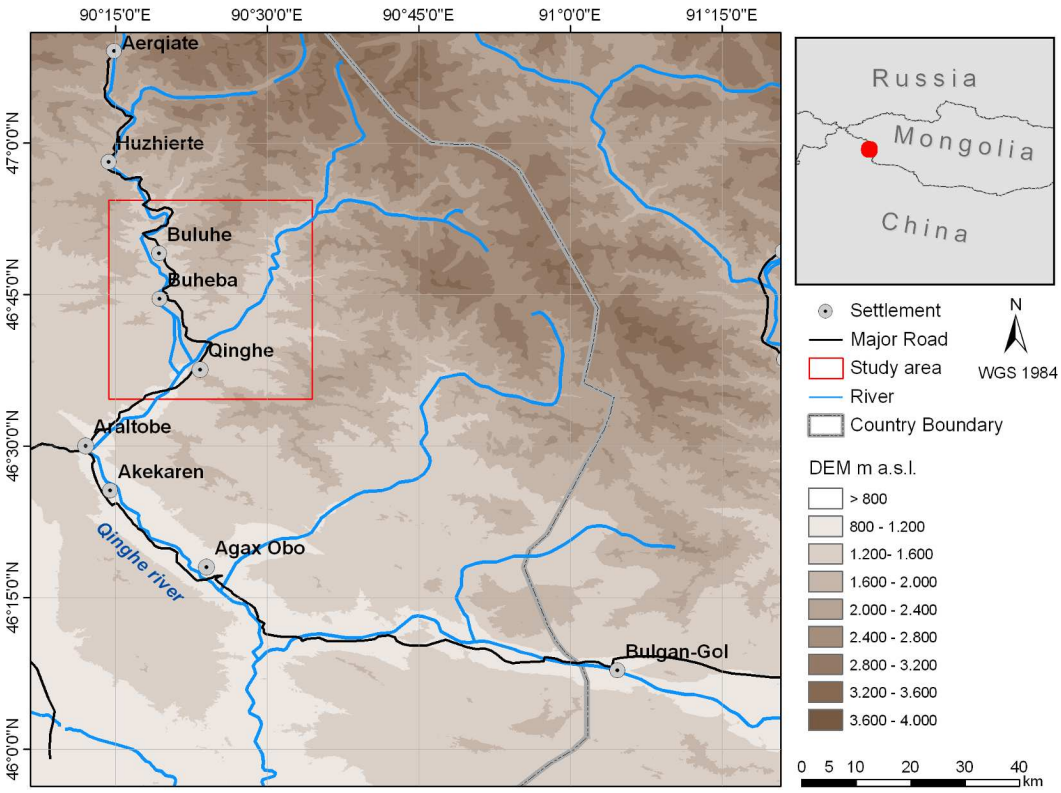

Fig. 1: *Location of the study area (482 km^2) in the Xinjiang autonomous region of NW China.*

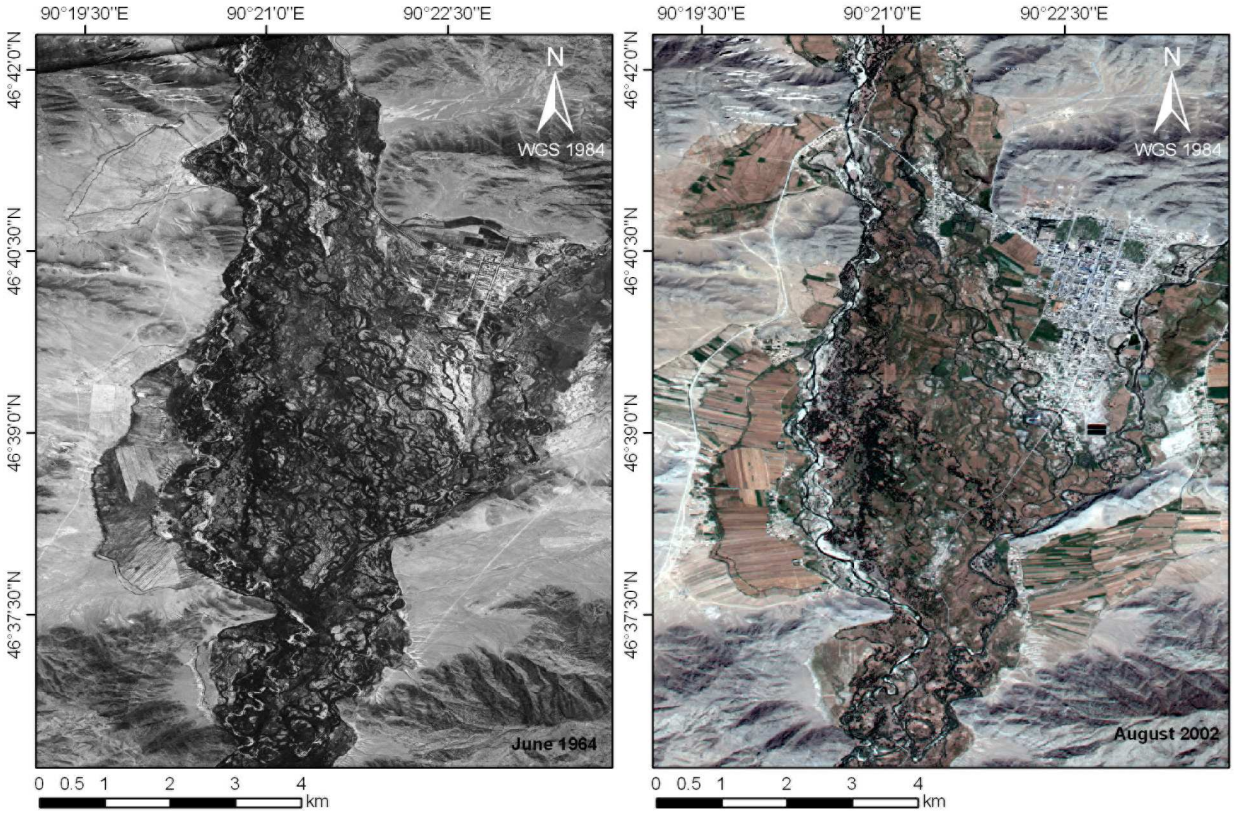

Fig. 2: *The oasis settlement Qinghe and its surrounding in June 1964 (Corona image) and August 2002 (Google Earth image).*

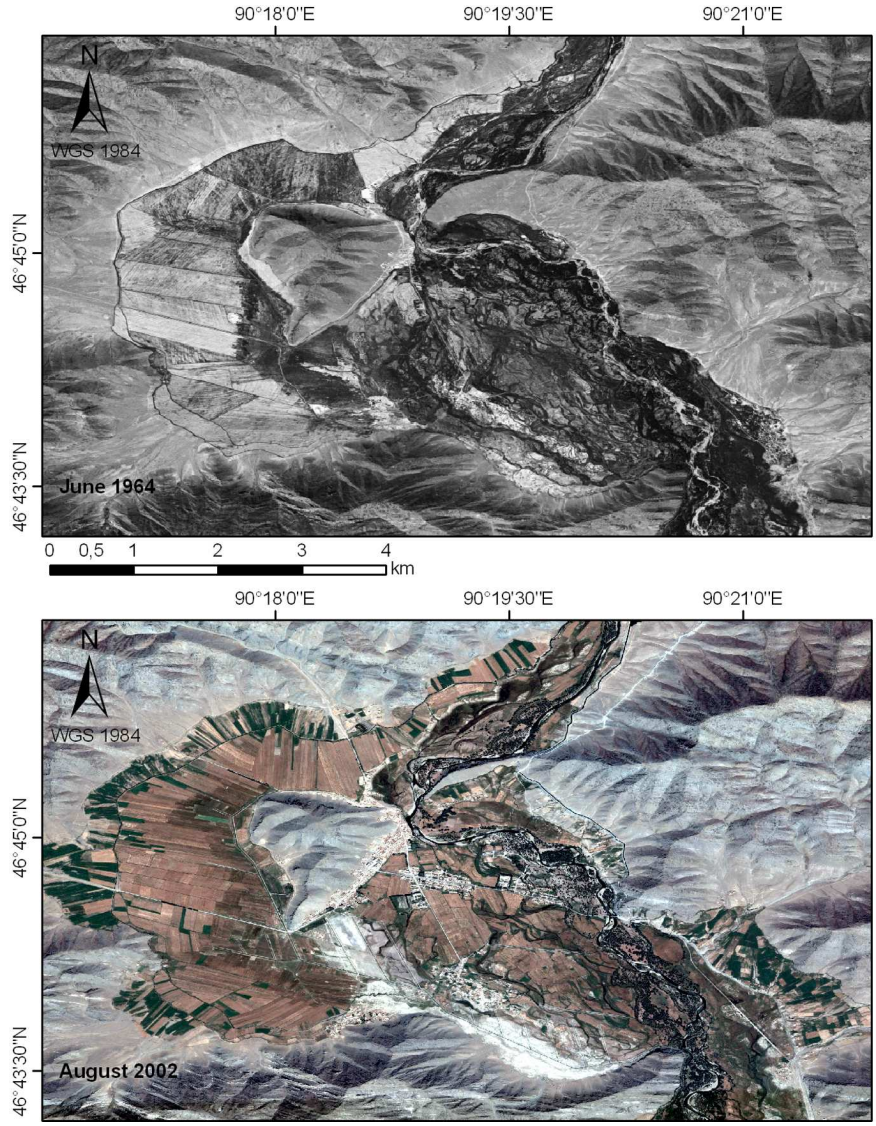

Fig. 3: *The oasis settlement Buheba and its surrounding in June 1964 (Corona image) and August 2002 (Google Earth image).*

Table 1: *Provider, date of acquisition and spatial resolution (m) of the satellite images used for LUCC analysis in the Dzungarian river basin, NW China.*

Satellite	*Provider*	*Date of Acquisition*	*Spatial Resolution (m)*
Corona KH-4B	U.S. Geological Survey's Earth Resources Observation an Science	22 June 1964	1.80-7.6
Landsat-5	U.S. Geological Survey's Earth Resources Observation an Science	7 September 1990	Band 1-5, 7: 28.5
Landsat-7	U.S. Geological Survey's Earth Resources Observation an Science	16 August 1999 8 August 2008	Band 1-5, 7: 30; Band 8: 15 Band 1-5, 7: 25; Band 8: 12.5
TerraSAR-X	German Aerospace Center	May 2007	0.75
Google Earth®	Geocentre Consulting	20 August 2002 21 October 2006	<1 <1

All Landsat images have been co-registered to the radar and the Google Earth® images, which have been correctly georeferenced according to ground control measurements. The scanned Corona images were georeferenced using readily recognizable features such as roads and stone formations as ground control points and verifying the results based on georeferenced topographic maps and satellite images (Number of GCPs: 33 and 25; Root mean square error: 0.00002 and 0.00014; Transformation: Spline and 3rd Order Polynomial).

The available TerraSAR-X images were used to create a high resolution image containing the spectral information of the 2008 Landsat dataset to identify training and validation sites for the subsequent classification processes. One common problem in images acquired with the SAR technique, is the so called 'Speckle Effect' hindering a proper interpretation of these images (Oliver & Quegan, 2004). For speckle noise reduction a combination of the Enhanced Frost Filter and the Local Sigma Filter was applied using ENVI 4.2. (Research Systems, Boulder, CO, USA). The fusion step of the HSV transformed Landsat colour composites and the TerraSAR-X images were processed based on the 'Principal Component' technique (Pohl, 1999) using ERDAS IMAGINE 8.3. (Leica Geosystems GIS & Mapping LLC., Norcross, GA, USA).

2.3 Data analysis and classification methods

For the supervised classification of the Landsat datasets a 'Maximum Likelihood Classifier' (MLC) with subsequent smoothing and a 'Sequential Maximum A Posteriori Classifier' (SMAPC) were compared using the open source software Quantum GIS 0.11.0 'Metis' with the GRASS plugin (Quantum GIS Development Team, 2009). The MLC is a simple pixel based method which is often used for land use change detections (Pal & Mather, 2003; Booth & Oldfield, 1989). The subsequent smoothing reduces the so called 'salt and pepper' effect characterized by scattered single pixels belonging to another class than the majority of the neighbouring pixels (Lillesand & Kiefer, 2000) and was applied to improve the classification results. In its classification the SMAPC also accounts for the spatial information between neighbouring pixels and produces more homogenous regions than obtained with the pixel-by-pixel method which computes local image pyramids at different scales (Bouman & Shapiro, 1994; McCauley & Engel, 1995). At each scale the best segmentation is calculated based on the previous coarser segmentation and the observed data using a spectral class model known as Gaussian mixture distribution (Bouman & Shapiro, 1994).

Based on field observations and visual inspections of recent Google Earth® images, different land use classes were detected within the study area (Table 2). The class 'Urban Areas' included all man-made facilities such as houses in the countryside and bigger settlements as well as industrial facilities. Water bodies were defined as class 2 and riverbanks as class 3. The latter were situated next to the water bodies, and were defined as a separate class to avoid misclassifications with other ground objects such as pathways or eroded land. To observe the development of the agriculturally used land classes 4 to 6 were defined based on spectral and spatial information such as the appearance of irrigation channels and the more or less rectangular shape of the fields as additional criteria. These areas were further discriminated according to their status (harvested-not harvested-degraded). Areas with soil degradation due to soil salinity were identified to (i) investigate how many areas were already degraded and (ii) determine the extent to which degraded arable land was reclaimed into pasture and forest land. The non-agricultural areas within the floodplain of the oases are typically characterised by woodlands (natural riverside forest of *Populus diversifolia* and plantations with *Populus alba*) and grasslands used for haymaking and grazing.

The non-vegetated and/or unutilized areas within and outside the oases were allocated to class 9 ('Mountains') and the vegetated areas in the proximity of the oases to class 10 ('Rangelands'). The definition of these classes allowed the analysis of grazing effects on rangeland areas.

To determine specific spectral reflectance patterns for the supervised classification (Lillesand & Kiefer, 2000; Sabins, 1997), training sites were defined for each class based on the pan-sharpened Landsat image of 2008. Subsequently, a signature file with the specific spectral attributes for each class was calculated. A comparison of the Landsat histograms of the three different years (1990, 1999 and 2008), which display the distribution of the digital numbers (DN) representing the spectral reflection/absorption of the landscape (Wilkie & Finn, 1996), revealed spectral differences for the year 1990, whereas 1999 and 2008 were more or less similar (Figure 4).

It was therefore necessary to redefine the signature files for the older Landsat images by using additional training sites for 1990 and 1999. These have been visually identified using spectral information of pseudo-true colour and standard false colour composites, whereby the visual interpretation was calibrated based on already known spectral and shape characteristics (colour, structure, size) of the year 2008. Finally, the mean of the spectral reflectance patterns was calculated for each class in 2008, 1999 and 1990 and compared among years.

For the oasis area (class 1 to 9) a supervised classification was conducted, whereby the surrounding rangeland area was further classified using the Normalized Difference Vegetation Index (NDVI) based on the Landsat images. The NDVI is the ratio of the reflectance in

Table 2: *Predefined land use classes, number and total area (ha) of training sites (TS) and validation plots (VP) for the supervised classification of LUCC in the Dzungarian river basin, NW China.*

Class Number	*Class Name*	*Ground Objects*	*Number and size of TS*	*Number and size of VP*
1	Urban Areas	single houses, settlements, cities, industrial facilities	428 (7.0)	393 (7.2)
2	Water Bodies	main river, branches, reservoirs	90 (7.0)	50 (4.3)
3	Riverbanks	sandy areas next to class 2	54 (1.9)	45 (2.9)
4	Agricultural Land–Harvested	arable land (signs of soil cultivation) harvested	78 (32.9)	65 (21.7)
5	Agricultural Land–Crops	arable land (signs of soil cultivation) not harvested	110 (29.3)	96 (27)
6	Agricultural Land–Degraded	arable land (signs of soil cultivation) degraded due to soil salinity	68 (27.7)	46 (5.5)
7	Floodplain–Wood	woodland in the floodplain	69 (24.3)	66 (26.0)
8	Floodplain–Meadow	grassland and bushes in the floodplain	49 (39.7)	51 (15.8)
9	Mountains	non-vegetated areas, blank soil, rocks within and outside the oasis	56 (139.8)	51 (124.0)
10	Rangelands	vegetated areas (grassland, bushes, trees) in the proximity of the oasis	– †	128 (43.4)

† Classification based on NDVI thresholds only without the use of training sites

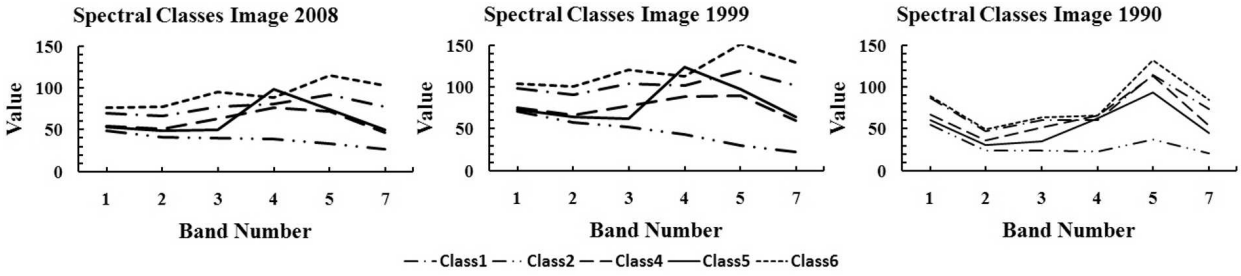

Fig. 4: *Means of the spectral reflectance patterns of the five most important land use/land cover classes used for supervised classification for the Landsat images of the Dzungarian River Basin, NW China, in 2008, 1999 and 1990.*

the near-infrared (NIR) and red (RED) portions of the electromagnetic spectrum (Tucker, 1979), and is calculated as $NDVI = (NIR - RED)/(NIR + RED)$. NDVI values ≥ 0.05 were used to separate between vegetated (class 10 = Rangeland) and non-vegetated rangeland areas (class 9 = Mountains).

To classify the panchromatic, historical Corona images a visual image interpretation was conducted (Antrop & Van Eetvelde, 2000). An automatically object oriented classification approach did not generate satisfactory results, mainly because of the high heterogeneity in size, shape and colour of the ground objects within the classes (such as small irregular shaped agricultural fields within the floodplains versus nearly quadrate fields outside the floodplains) and similar characteristics of ground objects belonging to different classes (irregular spaced patches of grassland and arable land in the floodplains). Some ground objects were too small to be separated from neighbouring objects such as single houses next to trees.

Since the detection of differences in vegetation cover is impossible in panchromatic data sets, vegetated and

non-vegetated areas within the rangelands were not separated for the Corona images. Furthermore, classes 4 and 5 were combined to one class as it was not detectable whether agricultural land was already harvested or not. Since salinity affected areas generally appear brighter than undisturbed agricultural land (Jensen, 2007), we further reclassified very bright areas of the agricultural land (raster value > 225) to degraded land.

Visual inspections of the panchromatic Corona image revealed, that some agricultural areas were located on marginal sites characterised by shallow soils wich restricted the water holding capacity. The interpretation was based on the relief condition using a Digital Elevation Model (NASA's Shuttle Radar Topography Mission; resolution = 90m) as ancillary information and the spectral properties of the image, whereby dry soils generally cause a higher reflectance compared to wet soils (Wilkie & Finn, 1996). Since we expected land abandonment to particularly occur in these areas, the land use changes of the marginal agricultural areas were examined separately in an additional step of analysis (Table 6).

2.4 Accuracy assessment

To identify the most suitable classification method for the study area, an accuracy assessment was conducted based on independent validation plots (Table 2) gathered from high resolution images and own field observations. Since no historical high resolution images were available, accuracy assessment using the 'kappa-coefficient' and an 'error matrix' (Congalton & Green, 1999) was only feasible for the year 2008. Based on the error matrix the Producer's Accuracy (PA), the Consumer's Accuracy (CA), the Error of Omission (EO) and the Error of Commission (EC) were calculated. The PA is a measure to assess how correctly classes were classified, whereas the CA reflects how reliable a classified map is. The EO indicates which areas were wrongly excluded from a class and the EC is a measure of which areas were wrongly included in a class (Campbell, 2002). The reference data (Congalton & Green, 1999) for class 1 to 8 were identified using the pan-sharpened Landsat image of 2008. For the classes 9 to 10 we used a HSV transformed 'standard false colour' composite of the 2008 Landsat dataset, suitable to discriminate vegetated and non-vegetated areas (Sabins, 1997).

2.5 Post processing

For the most suitable classifier (Table 4), the classified Landsat data were post-processed to further improve classification accuracy. Some classes had similar spectral characteristics, resulting in a high error of confusion, particularly, non-vegetated mountainous regions, urban areas, riverbanks and degraded agricultural land. During post-processing the urbanized and agriculturally used oasis areas were reclassified. The pan-sharpened Landsat, the Google Earth® and the historical Corona satellite images allowed to visually identify and digitize all urban areas from 1964-2008. Within this potential urbanization zone, all areas misclassified as 'Agricultural Land – Degraded' and 'Riverbanks' were reclassified as 'Urban Areas'. Outside this zone, some parts with sparsely vegetated arable land were misclassified as 'Urban Areas' and had thus to be reclassified as 'Agricultural Land – Crops'.

To correct further misclassification errors, we defined a zone of riverbanks along water streams using the buffer function of ArcGIS 9.3 (vers. 1.1; ESRI, Redlands, CA, USA). The location of the streams was defined through an automated extraction of the drainage network from the digital elevation model using the ArcHydro Tools contained in ArcGIS 9. According to visual inspections, the maximum extension of riverbanks next to the streams was around 75 m. Within this buffer zone all misclassified areas were reclassified into 'Riverbanks'. Outside this zone misclassified riverbanks were corrected into the class 'Agricultural Land – Degraded' (Table 3).

Table 3: *Identified region of reclassification, type of reclassification and extend of reclassified area (ha) for the post processing of the classified Landsat data (acquired in 1990, 1999 and 2008) in the Dzungarian river basin, NW China. For class abbreviations see Table 2.*

Region of Reclassification	*Type of Reclassification*	*Extend of the Areas (ha)*		
		1990	*1999*	*2008*
Inside urbanisation zone	Class 3 to Class 1	15	5	38
	Class 6 to Class 1	203	225	345
Outside urbanisation zone	Class 1 to Class 5	489	221	528
Inside zone of riverbanks	Class 1 to Class 3	127	38	222
	Class 6 to Class 3	19	49	25
	Class 9 to Class 3	90	97	67
Outside zone of Riverbanks	Class 3 to Class 6	67	60	84

3 Results

3.1 Reliability of the determined sets of training sites

Reliability of the determined sets of training sites For the Landsat images of the years 2008 and 1999 the means of the spectral patterns were similar indicating that the training sites were identified correctly (Figure 4). They are slightly shifted due to different minimum and maximum DN values. As the training sites for the 1990 Landsat dataset were identified in the same way as the 1999 data, we assumed that they were also identified correctly and that the differences of the spectral patterns are only due to differences of the DN distribution.

3.2 Accuracy assessment of the classification results

The validation of the produced maps of the 2008 data revealed that the best classification result was obtained using the SMAPC method (Table 4). The subsequent post processing to improve the accuracy of the classified urban areas and riverbanks increased the kappa coefficient from 0.90 to 0.92. The error matrices obtained pointed to a major reduction of errors due to the post processing (Table 5). Therefore this method was also used for the classification of the 1990 and 1999 data.

Table 4: *Accuracy assessment of the different classifiers (MLC = Maximum Likelihood Classifier; SMAPC = Sequential A Priori Classifier; Post Processing = post processing of the urban areas and riverbanks; Smooth = smoothing of the thematic map after classification and prior to the accuracy assessment) for the 2008 Landsat data used to examine LUCC in the Dzungarian river basin, NW China.*

Classifier	*Special Steps*	*Kappa - Coefficient*
SMAPC	–	0.8969
SMAPC	Post Processing	0.9209
MLC	Smoothing	0.8929

Some verified urban areas were misclassified as 'Riverbanks', 'Agricultural Land – Degraded' and 'Agricultural Land – Crops'. Post-processing, allowed to reduce errors and confusion between urban areas and riverbanks or degraded agricultural land. Therefore the PA for urban areas strongly improved (Table 5b).

The high EO of the class 'Riverbanks' was due to misclassifications in 'Urban Areas' and 'Mountains', and due to a confusion with agricultural land. Post-processing successfully diminished the former misclassification error, thereby improving the PA from 57 % to 91 %.

Even without post-processing, PA's and CA's of all classes were > 90 %. Lower accuracies were only observed for classes that depicted the more natural floodplain vegetation. The EO of these classes were mainly due to misclassifications among each other and the exclusion of areas misclassified as harvested or degraded agricultural land as well as riverbanks. The PA of the rangelands was < 90 % due to confusion with non-vegetated areas near the oases. Nevertheless, a very high CA of 100 % was achieved for this class, which was similar to the classes 'Urban Areas' and 'Water Bodies'.

3.3 Changes of the different classes by surface area

The urban areas constantly expanded from 285 to 814 ha in 1964 and 2008 respectively (+186 %, Table 6). The total agricultural land increased by 61 % and reached 6,834 ha in 2008. The highest increments occurred between 1990 (5,000 ha) and 1999 (6,400 ha). Compared to 1964, more land was classified as degraded agricultural land in the following years, whereas in 1990 a maximum of 1,180 ha was detected. From 1990 to 2008 degraded farmland, which was apparently affected by soil salinity decreased in size (630 ha). The area in the floodplain covered with trees decreased until 1999 (-45 %) compared to 1964, but expanded by 12 % since then. The grassland interspersed with bushes in the floodplain slightly increased by 3 % between 1964 and 1990 but decreased constantly in the following years, reaching a size of 1400 ha in 2008. The extent of the water bodies fluctuated over the years with a minimum of 280 ha and a maximum of 500 ha in 1964 and 1999 respectively. The total size of the oasis increased from 8,310 up to 9,160 ha during the studied time span. It could also be determined that the rangelands were about 60 km^2 smaller in 2008 than in 1990.

3.4 Land use changes of marginal agricultural areas

In 1964 around 19 % of the total agricultural land was located on marginal sites characterized by shallow soils and steep slopes. A small part of this land (5 %) was urbanised in the following years. The majority of this former agriculturally used land (30 %) was abandoned and classified as non-vegetated mountainous region in the years after 1964. Most of land abandonment occurred in 1990, whereby the agricultural use at marginal sites increased again in 1999 and 2008 by 760 ha up to 880 ha. Conversely, the size of degraded agricultural land increased from 240 ha in 1964 up to 490 ha in 1990 and declined until 2008, reaching an extent of 180 ha (Table 7).

4 Discussion

4.1 LUCC in oases settlements and surrounding rangelands

Overall, the trends of LUCC in mountain oases of the present study were largely similar as compared to steppe and deserted regions of northern China with decreasing areas of grasslands and degraded land and expanding

urban areas as well as farmlands (Li *et al.*, 2004; Luo *et al.*, 2008; Hao & Ren, 2009; Yu *et al.*, 2010). The total size of the oasis settlements increased from 4,200 to 6,800 ha between 1964 and 2008. This expansion was accompanied by an over-intensification of agriculture (Zhu & Chen, 1994), and thus agricultural fields at marginal sites were abandoned simultaneously (around 400 ha). Urban areas constantly expanded from 280 to 810 ha in the examined time span. This corresponds to the population development of Qinghe county (Qinghe County Administration, unpublished) and of Xinjiang in the last decades (Wiemer, 2004). Furthermore, the agricultural area used for cropping increased in size along with a reduction of the floodplain area covered with trees, bushes and grassland. Since 1990, the grassland area decreased by 53 % while livestock numbers remained relative constant from 1997 to 2006 with a peak in 2000 (Qinghe County Administration, unpublished).

Table 5: *Error matrices (CA = Consumer's Accuracy; PA = Producer's Accuracy; EC = Error of Commission; EO = Error of Omission) of the land use classes identified by the validation plots within the study area in the Dzungarian River Basin of NW China. Data are based on the SMAPC classification results of the 2008 Landsat data before (a) and after (b) post-processing. For class abbreviations see Table 2.*

a)

		Ground Truth Data												
	Class	*1*	*2*	*3*	*4*	*5*	*6*	*7*	*8*	*9*	*10*	*Total*	*CA (%)*	*EC (%)*
Classified Map	*1*	119	3	28	0	24	4	2	1	0	0	181	65.8	34.2
	2	0	109	0	0	0	0	0	0	0	0	109	100.0	0.0
	3	19	1	47	1	0	1	0	1	0	0	70	67.1	32.9
	4	0	0	1	376	17	0	7	5	0	0	406	92.6	7.4
	5	14	0	1	4	495	7	14	6	0	0	541	91.5	8.5
	6	19	0	1	0	0	117	0	0	0	0	137	85.4	14.6
	7	0	0	0	0	0	0	441	38	0	0	479	92.1	7.9
	8	1	0	0	0	0	0	40	245	0	0	286	85.7	14.3
	9	0	1	4	0	0	0	0	0	1987	136	2128	93.4	6.6
	10	0	0	0	0	0	0	0	0	0	670	670	100.0	0.00
	Total	172	114	82	381	536	129	504	296	1987	809	5007		
	PA (%)	69.2	95.6	57.3	98.7	92.4	90.7	87.5	82.8	100.0	83.1			
	EO (%)	30.8	4.4	42.7	1.3	7.6	9.3	12.5	17.2	0.0	16.9			

b)

		Ground Truth Data												
	Class	*1*	*2*	*3*	*4*	*5*	*6*	*7*	*8*	*9*	*10*	*Total*	*CA (%)*	*EC (%)*
Classified Map	*1*	157	0	0	0	0	0	0	0	0	0	157	100.0	0.0
	2	0	109	0	0	0	0	0	0	0	0	109	100.0	0.0
	3	0	4	75	0	0	0	1	1	0	0	81	92.6	7.4
	4	0	0	1	376	17	0	7	5	0	0	406	92.6	7.4
	5	14	0	3	4	519	11	15	7	0	0	573	90.6	9.4
	6	0	0	3	1	0	118	0	0	0	0	122	96.7	3.3
	7	0	0	0	0	0	0	441	38	0	0	479	92.1	7.9
	8	1	0	0	0	0	0	40	245	0	0	286	85.7	14.3
	9	0	1	0	0	0	0	0	0	1987	136	2124	93.6	6.4
	10	0	0	0	0	0	0	0	0	0	670	670	100.0	0.0
	Total	172	114	82	381	536	129	504	296	1987	806	5007		
	PA (%)	91.3	95.6	91.5	98.7	96.8	91.5	87.5	82.8	100.0	83.1			
	EO (%)	8.7	4.4	8.5	1.3	3.2	8.5	12.5	17.2	0.0	16.9			

Table 6: *Post classification comparison showing the area (ha) of the different land uses classes in the Dzungarian river basin, NW China (1964 – 2008). Calculated changes refer to 1964 for the classes of the oasis settlements and on 1990 for the classes of the periphery.*

Class	1964	1990		1999		2008	
	Area	Area	Changes (ha & %)	Area	Changes (ha & %)	Area	Changes (ha & %)
Urban Areas	285	646	361 (+127)	706	421 (+148)	814	529 (+186)
Water Bodies	280	344	65 (+23)	505	226 (+81)	366	86 (+31)
Riverbanks	69	258	189 (+272)	145	76 (+109)	333	264 (+381)
Agricultural Land-Harvested	3692	2583	–	1875	–	2668	–
Agricultural Land-Crops		1226	–	3802	–	3534	–
Agricultural Land-Degraded	544	1184	640 (+118)	720	176 (+32)	632	88 (+16)
Total Agriculture	*4236*	*4993*	*757 (+18)*	*6397*	*2161 (+51)*	*6834*	*2598 (+61)*
Floodplain – Forest	1402	840	-562 (-40)	773	-629 (-45)	868	-534 (-38)
Floodplain – Meadow	2676	2763	87 (+3)	1749	-927 (-35)	1455	-1221 (-46)
Total Oases	*8314*	*8596*	*282 (+3)*	*8919*	*605 (+7)*	*9158*	*843 (+10)*
Mountains	–	27452	–	29210	1758 (+6)	32590	5138 (+19)
Rangeland	–	10860	–	8672	-2188 (-20)	4902	-5958 (-55)
Total Area	*8314*	*48156*	–	*48157*	–	*48162*	–

Table 7: *Surface area (ha) and changes of cultivated and degraded agricultural land at marginal sites within oasis settlements in the Dzungarian river basin, NWt China (1964 – 2008). 'Cultivated' refers to agricultural land harvested as well as covered with crops.*

Class	1964	1990		1999		2008	
	Area	Area	Changes (ha & %)	Area	Changes (ha & %)	Area	Changes (ha & %)
Cultivated Agricultural Land	1346	545	-801 (-60)	760	-586 (-44)	880	-466 (-35)
Degraded Agricultural Land	236	492	255 (+108)	290	53 (+23)	183	-54 (-23)

During winter times livestock is kept in the floodplains and the fodder mainly consists of hay and wheat straw (Banks, 2001). Thus, it can be assumed that the importance of grasslands as potential fodder source declined while crop residues (available at larger scales) became more important. The proportion of the area classified as degraded agricultural land decreased from nearly 1,200 to 600 ha in 1990 and 2008 respectively; whereas the level of degraded land was higher compared to 1964. This indicates that the policy for reconverting degraded land into pasture or forest land is already producing measurable results. The expansion of woodland in the floodplain by 12 % from 1999 to 2008 resulted from reforestation efforts started in 2002. Management improvements have been undertaken as well to avoid soil salinity and to reclaim degraded areas for agricultural useas reported for other regions in northern China (Yu *et al.*, 2010).

However, the differences in the acquisition dates of the Landsat datasets may also be a reason for the decrease of degraded land. The Landsat image of 1990 was recorded one month later and thus around 20 % more land was already harvested compared to 1999 and 2008. As a result, more agricultural land was without vegetation cover including land affected by low soil salinity. These areas were not classified as degraded in the images of 1999 and 2008, which were acquired one month earlier, since the spectral information of the cropped areas confounded the information of the soil salinity. For a more precise estimation of the total extent of saline soils, imagery with a large amount of bare soil taken outside the vegetation period during winter times would reveal better results.

After 1964 a bigger area on the images was classified as 'Water Bodies'. This accords well with the findings of Li *et al.* (2001) who reported that the water table

within the oasis systems has been raised due to the large scale application of irrigation water. The fluctuation of the amount of irrigation water can be explained by differences in the inflow of melt-water from the surrounding mountains, which feds most of the river systems in northern China (Banks, 2001).

According to the results in the present study, rangelands decreased by nearly 60 km^2 from 1990 to 2008. Generally, the reduction of rangeland areas in arid and semi-arid regions can be explained by two contrary models. One is the non-equilibrium model, whereby the extent and productivity of rangelands is mainly determined by precipitation (Sullivan & Rohde, 2002). The equilibrium model in contrast identifies overgrazing as a major cause for declining productivity and palatability of the rangelands, through a reduction of biodiversity and changes in species composition (Christensen *et al.*, 2003; Vetter, 2005). Overgrazing can make pasture land more susceptible to wind erosion resulting in a decline of rangeland areas (Baoping & Tianzong, 2001). For our study area, the causes for the degradation of rangeland areas remain unclear since precipitation data does not cover the whole time span and is only available until 1997 (NCDC, 2009). Furthermore, it was impossible to diminish inter- and intra-annual effects of precipitation based on monthly NDVI calculations (Richard & Poccard, 1998; Weiss *et al.*, 2001), due to a lack of sufficient Landsat datasets. Nonetheless, drought events have been detected for 1989 and 1990. That similar recurrent drought events caused the observed reduction in vegetation cover until 2008 is not very likely, indicating that overgrazing may also be responsible for the degradation of the rangelands as explained by the equilibrium model.

4.2 Evaluation of the conducted classification

Oasis systems in arid NW China are vulnerable micro ecosystems encompassed by very large rangeland areas. These two 'ecosystems' differ substantially in productivity and species composition as it has been reported for comparable regions in Mongolia (Hilbig & Tungalag, 2006). This is mainly due to differences in water availability. The productivity of oasis systems is based on irrigation water supplied by rivers fed by melt-water, the surrounding rangelands instead depend on scarce precipitation events (Banks, 2001; Wang & Cheng, 2000). Taking these characteristics into account, both ecosystems were classified separately to gather more accurate results for the analysis of LUCC. Furthermore, a prestudy revealed various misclassifications between vegetated rangeland areas and land use classes of oases (such as un-harvested agricultural land, grassland and bushes of the floodplain). However, the separation of oasis settlements and rangeland areas as an additional step during the classification process is time consuming, particularly on a broader scale.

The SMAPC and the MLC method with subsequent smoothing resulted in similar classification accuracies. The former performed slightly better which agrees with the findings of McCauley & Engel (1995) indicating that this classifier is more efficient for classifying different types of crops cultivated on homogenous fields. However, a post processing of the classified Landsat data was still necessary, as misclassification among urban areas, riverbanks, degraded agricultural land, and mountainous areas occurred frequently. The post processing of the classified Landsat datasets improved considerably the PA values of the classes 'Urban Areas' and 'Riverbanks' by 22 % and 34 %, respectively. Most of the land use classes were classified in an acceptable way with PA values > 90 %. On the other hand, post-processing slightly increased the error of confusion among riverbanks, degraded agricultural land as well as agricultural land covered with crops. Additionally, some woodland areas of the floodplains were misclassified as riverbanks and agricultural land after post-processing. The assumed zone of riverbanks used during post processing still depends on some uncertainties, whereby the real extent of riverbanks was under- as well as overestimated for some areas.

The use of ancillary information for a more powerful and accurate automated classification is recommended. For instance, Stefanov *et al.* (2001) used, among others, the results of a texture analysis for the identification of urban areas in a semi-arid region of Arizona, USA. They reported that the occurrence of houses, streets and paths caused more texture compared to homogenous agricultural fields. However, if a texture analysis successfully identifies small-scale structures in the present study (scattered houses in the floodplains, single bushes or trees) remains questionable. To quantify soil salinisation more precisely, a correlation analysis between reflectance spectra of the Landsat datasets and measured soil electric conductivity (EC) could be conducted. This would facilitate a better identification of areas potentially at risk of salinisation (Yu *et al.*, 2010).

The low classification accuracies and misclassifications among trees, grassland interspersed with bushes and agricultural used land can be explained by their similar reflectance characteristics, since all classes depict highly productive landscape features. Another reason is the patchy structure of the floodplains with small-scale changes of different land use types. These may enhance the classification of 'mixed pixels' containing the spectral information of different ground features (Wilkie & Finn, 1996). Hence, a fuzzy classification approach (Tso & Mather, 2001) would be more suitable to classify these floodplain areas. Since each ground object covered by one pixel contributes to the recorded brightness value, the brightness of mixed pixels changes slightly as the ratio of the covered ground objects vary. By means of fuzzy rules and weighting factors, the researcher can define in which range of brightness values

a mixed pixel should be dedicated as a member of a certain class (Tso & Mather, 2001). For instance, in the present study mixed pixels contained information from cultivated agricultural land and its surrounding vegetation (grass, bushes), whereat a corresponding range can be applied to intensify the weighing of cultivated land and finally assess the biggest extension of farmland.

The specified NDVI threshold of 0.05 to classify the studied rangelands revealed accurate classification results with a CA of 100 %. Wang *et al.* (2008) detected even lower NDVI values for vegetated areas within arid rangelands of NW China, but non-vegetated soils can generate also slightly higher values than 0.05. However, reddish areas in a standard false colour image of the 2008 Landsat dataset, indicating vegetation cover (Sabins, 1997), were mostly concurrent to areas characterised by NDVI values of 0.05 and higher.

For the panchromatic mode of the Corona images, cumbersome visual image interpretation was necessary, whereby harvested and non-harvested agricultural land as well as vegetated and no-vegetated rangelands could not be well differentiated and was thus not performed. Even though visual interpretations are time consuming, such methods facilitate the simultaneous processing of texture, grey-colour level tones and geometric features, and thus offer a rather accurate and realistic way of interpretation (Ruelland *et al.*, 2010). Furthermore, some observed land cover changes may be overestimated as a result of possible biases in post-classification comparison resulting from different classification approaches (visual interpretation of Corona images versus automatic classification of Landsat images).

5 Conclusions

Remote sensing methods for the analysis of landscape transformations processes are important monitoring tools in fast developing countries, such as Northern China, where dramatic land use changes occurred in the last 50 years. The current method used was adapted to the specific landscape characteristics of the present study area, whereas the SMAPC with subsequent post-processing revealed most accurate results. The extrapolation of this method is feasible for similar arid and semi-arid environments, but for a broad scale application the labour costs might be a limiting factor (digitizing urban areas per hand, separation of oasis from periphery), especially for the visual interpretation of Corona images. However, for the detection of small-scale changes within complex oasis systems this method gives more reliable and accurate results compared to standard classification methods.

The use of ancillary information during classification process such as a digital elevation model, precipitation data, agricultural statistics or the correlation between reflectance spectra of the Landsat datasets and measured soil electric conductivity is recommended to increase the classification accuracies of urban areas, abandoned land and degraded land.

Acknowledgements
The authors are indebted to Prof. Ximing Zhang for his tireless efforts in supporting the IFAD-funded WATERCOPE project (I-R-1284) in the transborder Altay-Dzungarian region of Mongolia and China.

References

Antrop, M. & Van Eetvelde, V. (2000). Holistic aspects of suburban landscapes: visual images interpretation and landscape metrices. *Landscape and Urban Planning*, 50, 43–58.

Banks, T. (2001). Property rights and the environment in pastoral China: evidence from the field. *Development and Change*, 32, 717–740.

Baoping, S. & Tianzong, F. (2001). Desertification in China and its control. In S. W. Breckle, M. Veste, & W. Wucherer (Eds.), *Sustainable Land Use in Deserts* (pp. 418–426). Springer, Heidelberg.

Booth, W. H. & Oldfield, R. B. (1989). A comparison of classification algorithms in terms of speed and accuracy after the application of a post-classification modal filter. *International Journal of Remote Sensing*, 10, 1271–1276.

Bouman, C. A. & Shapiro, M. (1994). A multiscale random field model for Bayesian image segmentation. *IEEE Transaction on Image Processing*, 3 (2), 162–177.

Bruelheide, H., Jandt, U., Gries, D., Thomas, F. M., Foetzki, A. & Buerkert, A. (2003). Vegetation changes in a river oasis on the southern rim of the Taklamakan Desert in China between 1956 and 2000. *Phytocoenologia*, 33, 801–818.

Brunner, P. A. (2005). *Water and salt management in the Yanqi Basin, China*. Ph.D. thesis Eidgenössische Technische Hochschule, Zürich.

Campbell, J. B. (2002). *Introduction to remote sensing, Third ed.*. Guilford Press, New York.

di Castri, F. & Hadley, M. (1988). Enhancing the credibility of ecology: Interacting along and across hierachical scales. *GeoJournal*, 17, 5–35.

Chander, G., Markham, B. L. & Helder, D. L. (2009). Summary of current radiometric calibration coefficients for Landsat MSS, TM, ETM+, and EO-1 ALI sensors. *Remote Sensing of Environment*, 113, 893–903.

Christensen, L., Coughenour, M. B., Ellis, J. E. & Chen, Z. Z. (2003). Sustainability of inner Mongolian grasslands: Application of the Savanna model. *Journal of Range Management*, 56, 319–327.

Chuluun, T. & Ojima, D. (2002). Land use change and carbon cycle in arid and semi-arid lands of East and Central Asia. *Science in China*, (Series C) 45, 48–54.

Congalton, R. G. & Green, K. (1999). *Assessing the accuracy of remotely sensed data. Principles and practices*. CRC Press, Boca Raton.

Gmaps Pedometer (2009). Calculation of the elevation. URL `http://www.gmap-pedometer.com/?r=2778274`.

Graefe, S., Siebert, S., Bruelheide, H. & Buerkert, A. (2004). Changes in the agricultural structure of the Qira-Oasis. In M. Runge, & X. Zhang (Eds.), *Contributions to a "Workshop on Sustainable Management of the Shelterbelt Vegetation of River Oases in the Taklimakan Desert". Urumqi 2003*. Shaker Verlag, Aachen.

Graetz, D. (1994). Grasslands. In W. Meyer, & B. L. Turner (Eds.), *Changes in land use and land cover, a global perspective* (pp. 125–148). Cambridge University Press, Cambridge.

Hao, H. & Ren, Z. (2009). Land use/land cover change (LUCC) and eco-environment response to LUCC in farming-pastoral zone, China. *Agricultural Sciences in China*, 8, 91–97.

Hilbig, W. & Tungalag, R. (2006). Vegetationskundliche Untersuchungen in der Borzongijn und Galbyn-Gobi (Ömnögov Aimak, Mongolei). *Feddes Repertorium*, 117, 399–426.

Hill, J. (2001). Remote sensing of surface properties. The key to land degradation and desertification assessments. In S. W. Breckle, M. Veste, & W. Wucherer (Eds.), *Sustainable land use in deserts* (pp. 243–254). Springer Verlag, Berlin.

Hu, Z.-Z., Yang, S. & Wu, R. (2003). Long-term climate variations in China and global warming signals. *Journal of Geophysical Research*, 108 (D19). doi: 10.1029/2003JD003651.

Jensen, J. R. (2007). *Remote sensing of the environment. An earth resource perspective. Second. ed.*. Pearson Prentice Hall, New York.

Jia, B., Zhang, Z., Ci, L., Ren, Y., Pan, B. & Zhang, Z. (2004). Oasis land-use dynamics and its influence on the oasis environment in Xinjiang, China. *Journal of Arid Environments*, 56, 11–26.

Jun, L., Shixin, W. & Xiaolei, Z. (2006). Temporal-spatial characteristics of the urbanization of rural land in Xinjiang. *Chinese Journal of Population, Resources and Environment*, 4, 37–44.

Klein, J. A., Harte, J. & Zhao, X. Q. (2004). Experimental warming causes and rapid species loss, dampened by simulated grazing, on the Tibetan Plateau. *Ecology Letters*, 7, 1170–1179.

Li, X., Fang, J. & Zhough, H. F. (2001). The hydrological effect under human activities in the inland watersheds of Xinjiang, China. *Chinese Geographical Science*, 11, 27–34.

Li, X. L., Yuan, Q. H., Wan, L. Q. & He, F. (2008). Perspective on livestock production systems in China. *Rangeland Journal*, 30, 211–220.

Li, Z., Li, X., Wang, Y., Ma, A. & Wang, J. (2004). Land-use change analysis in Yulin prefecture, northwestern China using remote sensing and GIS. *International Journal of Remote Sensing*, 25, 5691–5703.

Lillesand, T. M. & Kiefer, R. W. (2000). *Remote sensing and image interpretation. Fourth ed.*. Wiley, New York.

Liu, Y., Zhang, X., Lei, J. & Zhu, L. (2010). Urban expansion of oasis cities between 1990 and 2007 in Xinjiang, China. *International Journal of Sustainable Development and World Ecology*, 17, 253–262.

Liu, Y. M. (1993). Rangeland degradation in the pastoral region of China: causes and countermeasures. *ACIAR Techniqual Reports Series*, 25, 20–26.

Luo, G. P., Zhou, C. H., Chen, X. & Li, Y. (2008). A methodology of characterizing status and trend of land changes in oases: A case study of Sangong River watershed, Xinjiang, China. *Journal of Environmental Management*, 88, 775–783.

McCauley, J. D. & Engel, B. A. (1995). Comparison of scene segmentations: SMAP, ECHO and Maximum Likelihood. *IEEE Transactions on Geosience and Remote Sensing*, 33, 1313–1316.

Millward, J. A. & Tursun, N. (2004). Political history and strategies of control, 1978 – 2001. In S. F. Starr (Ed.), *Xinjiang - China's Muslim Borderland* (pp. 36–101). M.E. Sharpe Inc., Armonk, New York.

NCDC (2009). Climate data of the Qinghe/Qinglii station. URL `http://www1.ncdc.noaa.gov/pub/orders/CD07563271849103.txt`.

Oliver, C. & Quegan, S. (2004). *Understanding synthetic aperture radar images*. Sci-Tech Publishing, Raleigh.

Pal, M. & Mather, P. M. (2003). An assessment of the effectiveness of decision tree methods for land cover classification. *Remote Sensing of Environment*, 86, 554–565.

Pohl, C. (1999). Tools and methods for fusion of images of different spatial resolution. *International Archives of Photogrammetry and Remote Sensing*, 32, H. Part 7–4–3 W6.

Qinghe County Administration (unpublished). Data obtained from Qinghe County authorities in interviews in 2007.

Quantum GIS Development Team (2009). Quantum GIS (QGIS), Open Source Geospatial Foundation (OSGeo), GNU General Public License. URL `http://qgis.osgeo.org`.

Richard, Y. & Poccard, I. (1998). A statistical study of the NDVI sensitivity to seasonal and interannual rainfall variations in Southern Africa. *International*

Journal of Remote Sensing, 19, 2907–2920.

Ruelland, D., Levavasseur, F. & Tribotté, A. (2010). Patterns and dynamics of land-cover changes since the 1960s over three experimental areas in Mali. *International Journal of Applied Earth Observation and Geoinformation*, 12, Supplement 1, S11–S17. doi: 10.1016/j.jag.2009.10.006.

Runnström, M. C. (2003). Rangeland development of the Mu Us sandy land in semiarid China: an analysis using Landsat and NOAA remote sensing data. *Land Degradation & Development*, 14, 189–202.

Sabins, F. F. (1997). *Remote sensing. Principles and interpretation. Third ed.*. Freeman, New York.

Stefanov, L. W., Ramsey, M. S. & Christensen, P. R. (2001). Monitoring urban land cover change: an expert system approach to land cover classification of semiarid to arid urban centers. *Remote Sensing of Environment*, 77, 173–185.

Sullivan, S. & Rohde, R. (2002). On non-equilibrium in arid and semi-arid grazing systems. *Journal of Biogeography*, 29, 1595–1618.

Tso, B. & Mather, P. M. (2001). *Classification methods for remotely sensed data*. Taylor & Francis, London.

Tucker, C. J. (1979). Red and photographic infrared linear combinations for monitoring vegetation. *Remote Sensing of Environment*, 8, 127–150.

Turner, M. G., Gardner, R. H. & O'Neill, R. V. (2001). *Landscape ecology in theory and practise - Pattern and Process*. Springer, NY, Berlin, Hamburg.

Vetter, S. (2005). Rangelands at equilibrium and non-equilibrium: recent developments in the debate. *Journal of Arid Environments*, 62, 321–341.

Wang, G. & Cheng, G. (2000). The characteristics of water resources and the changes of the hydrological process and environment in the arid zone of northwest China. *Environmental Geology*, 39, 783–790.

Wang, R., Fan, Z., Zhang, H., Chen, Y. & Ma, Y. (2002). Remote sensing analysis of desert vegetation and its landscape changes: The case in middle reaches of Tarim River Basin, Xinjiang, China. *Science in China*, (Series D), 54–58.

Wang, S., Liu, S., Wang, X., Guo, J., Shuai, Y. & Hu, N. (2008). A simple method for information extraction of farm field in Tarim River Basin using MODIS data. *The International archives of the Photogrammetry, Remote Sensing and Spatial Information Sciences*, 37, 1043–1046.

Weiss, E., Marsh, S. E. & Pfirman, E. S. (2001). Application of NOAA-AVHRR NDVI time-series data to assess changes in Saudi Arabia's rangelands. *International Journal of Remote Sensing*, 22, 1005–1027.

Wiemer, C. (2004). The economy of Xinjiang. In S. F. Starr (Ed.), *Xinjiang - China's Muslim Borderland* (pp. 163–189). M.E. Sharpe Inc., Armonk, New York.

Wilkie, D. S. & Finn, J. T. (1996). *Remote sensing imagery for natural resources monitoring. A guide for first-time users*. Columbia University Press, New York.

Xiaoa, J., Shen, Y., Ge, J., Tateishi, R., Tang, C., Liang, Y. & Huang, Z. (2004). Evaluating urban expansion and land use change in Shijiazhuang, China, by using GIS and remote sensing. *Landscape and Urban Planning*, 75, 69–80.

Xiuling, F. S. C. (2001). Rationally utilizing water resources to control soil salinity in irrigation districts. In D. E. Stott, R. H. Mohtar, & G. C. Steinhardt (Eds.), *Sustaining the global farm, selected papers from the 10th International Soil Conservation Organization Meeting* (pp. 1134–1138). Purdue University and USDA-ARS National Soil Erosion Research Laboratory.

Yu, R., Liu, T., Xu, Y., Zhu, C., Qu, Z., Liu, X. & Li, C. (2010). Analysis of salinisation dynamics by remote sensing in Hetao Irrigation District of North China. *Agricultural Water Management*, 97, 1952–1960.

Zhang, K., Yu, Z., Li, X., Zhou, W. & Zhang, D. (2007). Land use change and land degradation in China from 1991 to 2001. *Land Degradation and Development*, 18, 209–219.

Zhang, X., Li, X. & Zhang, H. (2001). The control of drift sand on the southern fringe of the Taklamakan Desert and example from the Cele-oasis. In S. Breckle, M. Veste, & W. Wucherer (Eds.), *Sustainable land use in deserts* (pp. 350–356). Springer, Heidelberg.

Zhu, Z. D. & Chen, G. T. (1994). *Sandy Desertification in China. Status and Trends*. China Science Press, Beijing. 250pp. (in Chinese).